Korean J. of Chem. Eng., **12**(2), 258-263 (1995)

HEAT TRANSFER CHARACTERISTICS IN LOW-TEMPERATURE LATENT HEAT STORAGE SYSTEMS USING SALT HYDRATES

Jong Chan Choi*, Sang Done Kim† and Gui Young Han**

Department of Chemical Engineering, Korea Advanced Institute of Science and Technology, Taejon, Korea
*Samsung Engineering Co., Ltd., Seoul, Korea
**Department of Chemical Engineering, SungKyunKwan University, Suwon, Korea
(Received 22 September 1994 • accepted 28 October 1994)

Abstract—Heat transfer characteristics of a low temperature latent heat storage system have been determined for the circular finned and unfinned tubes using sodium acetate trihydrate as a phase change material (PCM). In the heat storage stage (melting process), the PCM heat transfer coefficient in the unfinned-tube system showed good agreement with the calculated value by the heat conduction equation. The heat transfer between the tube wall and the PCM was not enhanced by the fins in the thin-finned-tube system, whereas 2 times higher heat-transfer coefficient for the thick-finned-tube system over the unfinned-tube system was obtained. The experimentally determined heat-transfer coefficients in the unfinned-tube and thick-finned-tube systems are in the ranges of 40-170 and 80-320 W/m^2-k, respectively. The amount of heat storage for three systems has been correlated in terms of Fourier, Stefan and Reynolds numbers. The thermal performance of heat storage systems are found to be strongly dependent on the inlet temperature of heat transfer fluid.

Key words: *Thermal Storage Systems, Phase Change Material (PCM), Heat Transfer Coefficients, Supercooling, Phase Separation, Unfinned-tube System, Thick Finned-tube System*

INTRODUCTION

The development of energy storage systems has been increasingly important as a nationwide energy shortage makes effective use of available energy essential. The thermal energy storage has received considerable attention in the last several decades. Among the major three modes of thermal energy storage systems; sensible, latent and thermochemical, latent heat storage system using PCM has been studied extensively due to higher heat storage capacity and heat recovery at almost constant temperature during the phase change.

Latent heat storage system refers to a heat storage of latent heat from the PCM that undergoes solid-liquid or solid-solid phase transition. The low temperature latent heat storage system under 100℃ has been applied to residential heating and air conditioning [Lane, 1986]. In order to find better latent heat storage materials, numerous research works have been performed using inorganic salt hydrates [Abhat, 1983; Shin, 1989]. However the information on heat transfer is insufficient for the optimal design of latent heat storage system.

This present paper details heat transfer characteristics for different tube geometries and inlet temperatures of heat transfer fluid. Quantitative results are presented in terms of heat storage rates, heat transfer coefficient and thermal performance of energy storage system.

EXPERIMENTAL

The test facility used in this experiment is shown in Fig. 1. This system consists of heat storage unit, heat-transfer fluid

†To whom all correspondence should be addressed.

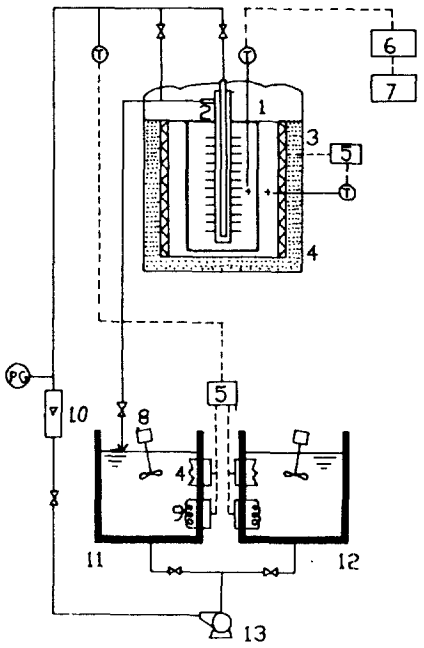

Fig. 1. Schematic diagram of the apparatus for low temperature LH-TES system.

1. TES vessel
2. Heat transfer tube
3. Electric heater
4. Insulating material
5. Temperature controller
6. Temperature recorder
7. Personal computer
8. Agitator
9. Cooler
10. Flowmeter
11. Hot water bath
12. Cold water bath
13. Pump

Table 1. Thermophysical properties of CH_3COONa-$3H_2O$

Peritectic point	58℃
Heat of fusion	226 (206) kJ/kg
Heat of formation (25℃)	−1.603 MJ/mol
Specific heat	
liquid	- (3.68) kJ/kg-K
solid	2.79 (2.11) kJ/kg-K
Thermal conductivity	
solid	- (0.6) W/m-K
Density	
liquid, 58℃	1.28×10^3 kg/m^3
solid	1.45×10^3 kg/m^3
Molecular weight	136.08 g/mol
percent salt	60.28 wt%
percent water	39.72 wt%

( ): properties with additives [Ryu et al., 1992]

(HTF) supply system and data recording devices. Sodium acetate trihydrate (CH_3COONa-$3H_2O$) was employed as a heat storage material. A mixture of 2 wt% carboxymethyl cellulose-Na (CMC-Na) and 1 wt% super-absorbing polymer is added in order to prevent undesirable phase separation of the PCM. Potassium sulfate (K_2SO_4) also used to reduce the supercooling of PCM during the freezing process (heat recovery stage) by 2 wt% as a nucleating agent. The detailed thermophysical properties of sodium acetate trihydrate with additives are given in Table 1.

The cylindrical latent heat storage vessel is made of stainless steel (74 mm i.d.×530 mm high×1.0 mm thick). The heat-transfer tube was constructed from a double tube of stainless steel (outer tube: 19.05 mm o.d.×480 mm long×0.5 mm thick; inner tube: 13.5 mm o.d.×480 mm long×0.5 mm thick) so that water as HTF flows in through the inner tube and flows out through the annulus between the inner and outer tube. In order to reduce the thermal resistance of HTF side, a helical type silicon wire was inserted as a turbulence promoter. Twelve circular fins of a stainless steel (60 mm fin dia.×19.05 mm fin-root dia.×0.4 mm thick for the thin-finned system, 3.0 mm thick for the thick-finned system) are welded on the outer surface of heat-transfer tube with 40-mm axial pitch. The total weight of the PCM was 2.6 kg with a heat storage capacity of 530 kJ, considering the latent heat only. In the heat storage material, fifteen 0.25-mm dia. Copper-constantan thermocouples (T-type, 30 AWG) are installed to measure the local temperatures at respective positions. Five same type thermocouples are soldered to measure the temperatures of heat transfer tube surface at different axial location. Since the setting length of each thermocouple wire in the radial direction along the circumference is at least 40 times larger than the wire diameter from the junction of the thermocouple, the heat intrusion to the junction caused by the temperature gradient within the wire is suppressed and the resultant error is minimized as Yanadori and Masuda [Yanadori and Masuda, 1989] recommended. The amount of heat transferred from the heat transfer tube to the heat storage material is calculated from the water flow rate and temperature difference. The water flow rate is measured with a calibrated rotameter and the temperatures of inlet and outlet of water are measured by two 0.25-mm dia. copper-constantan thermocouples. The temperature variation of each position was measured and recorded in a personal computer through a data acquisition system every one minute interval. In this experiment, after all PCM had been completely frozen, the initial temperature of PCM was set as 5℃ lower than the melting temperature of the PCM by adjusting three separate heaters inputs to make uniform temperature of the PCM in the container. In order to investigate the heat transfer effect on the heat storage with fluid inlet temperature and flow rate, wide ranges of operating conditions are employed. The specification of the experimental apparatus and conditions is summarized at Table 2.

Table 2. Specifications of the low-temperature latent heat storage system using CH_3COONa-$3H_2O$

Heat storage vessel
- Dimension : 74 mm-i.d.×530 mm-high×1.0 mm-thick
- Material : stainless steel

Heat transfer tube
- Outer tube : 19.05 mm-o.d.×480 mm-long×0.5 mm-thick
- Inner tube : 13.5 mm-o.d.×480 mm-long×0.5 mm-thick
- Circular fin : 60 mm over-fin dia.×19.05 mm fin-root dia.×40 mm-pitch, 0.4 and 3.0 mm-thick
- Material : stainless steel

Thermocouples
- Type : 0.25 mm dia.-copper constantan (T-type, AWG 30)
- Sheath : 2.0 mm-o.d.
- Junction position
  - PCM-radial 20, 30, 37 mm at 240 mm-axial distance
  - axial 0, 120, 240, 360, 480 mm at the tube wall
  - axial 0, 80, 160, 320, 400, 480 mm at 20 mm-radial distance
  - axial 0, 120, 360,480 mm at 37 mm-radial distance
- HTF-at inlet and outlet
- Data logging
  - Temperature recorder (Molytek 2702) and IBM-AT computer

Experimental conditions
- Phase-change material (PCM)
  - Composition-CH_3COONa-$3H_2O$: K_2SO_4: CMC-Na: SAP (95 : 2 : 2 : 1 wt%)
  - Capacity-2.6 kg (530 kJ)
- Heat Transfer Fluid (HTF) : city water
- Initial temperature of PCM : 53℃
- Inlet temperature of HTF, T_i (℃) : 68, 76, 84, 92
- Flow rate of HTF, m (g/min) : 200, 400, 600, 800

RESULTS AND DISCUSSION

1. Heat Storage Rates

The effect of inlet heat-transfer fluid temperatures and flow rates on heat storage rates is shown in Figs. 2, 3, and 4 for three different heat-transfer tube geometries. As can be seen in the Figs., the rates of heat storage for three types of geometries sharply decrease in the initial stage of heat storage and slowly decrease for the rest of heat storage stage at a given time interval. Of inlet HTF temperature, the higher inlet temperature showed higher rates of heat storage due to the increased driving force of heat transfer but the effect of the flow rate on heat storage rate was not significant. The minor effect of flow rate on the heat storage rate may be due to the turbulence promoter of helical wire inserted in the heat transfer tube. Because the flow of HTF

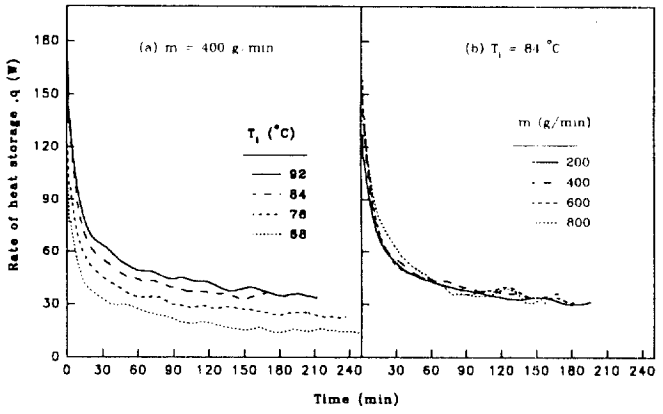

Fig. 2. Rate of heat storage in the unfinned-tube system.

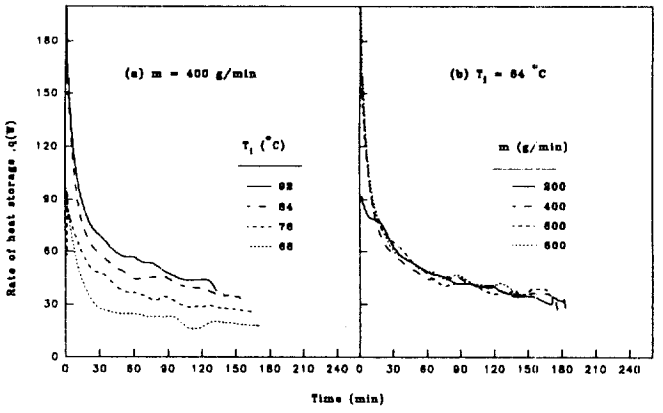

Fig. 3. Rate of heat storage in the thin-finned-tube system.

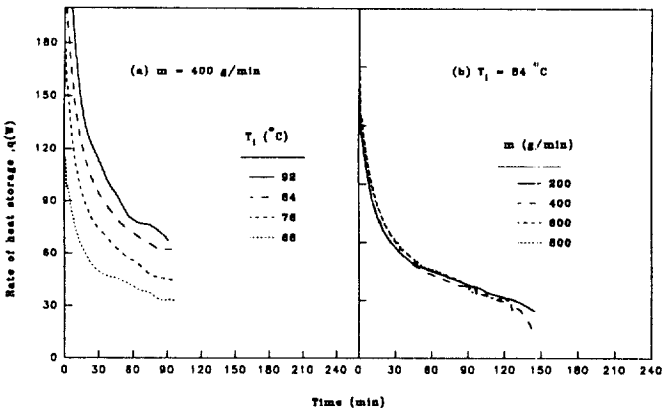

Fig. 4. Rate of heat storage in the thick-finned-tube system.

in the tube is already extremely turbulent even at the low flow rate owing to added turbulence promoter, the increased flowrate (increased Reynolds number) is less important.

Fig. 5 shows the comparison of heat storage rate in three different geometries systems at the same operating condition of inlet fluid temperature of 92℃ and flow rate of 400 g/min. From the Fig. 5 it can be said that the thin-finned-tube does not much increase the rate of heat storage over the unfinned-tube. However the thick-finned-tube system shows about 70% increase of rate of heat storage compared with the unfinned-tube system. This experimental finding may imply that there is a minimum fin thick-

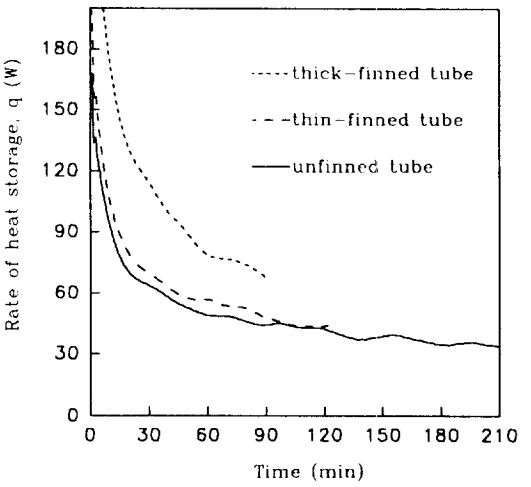

Fig. 5. Comparison of heat storage rate for the three systems.

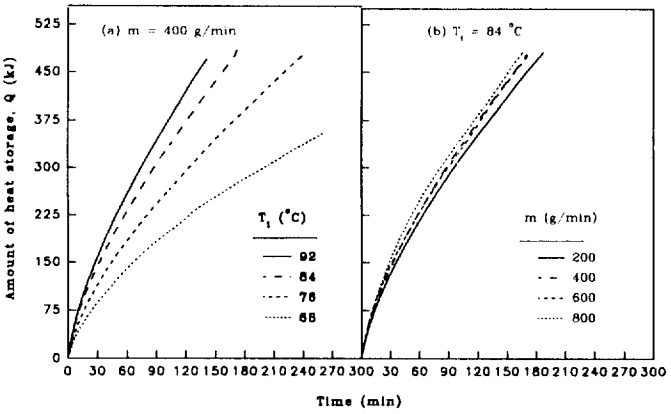

Fig. 6. Amount of heat storage in the unfinned-tube system.

ness for enhancing the heat transfer. The effect of fin geometry on heat transfer should be studied in detail for the optimal design of thermal heat storage system.

The cumulative amount of heat storage in the unfinned-tube system with respect to time is given in Fig. 6. As was discussed earlier, heat storage rates strongly depend on the inlet temperature of HTF and storage rates are independent on the flow rate. The amount of heat storage increases monotonically with time and there is no transition point that was found in this experiment of heat recovery stage (freezing process) due to the supercooling of PCM.

2. Heat-Transfer Coefficient

The variation of heat transfer coefficient (h_o) between the PCM and the heat-transfer tube surface with time (in terms of total amount of heat storage) for the unfinned-tube system is shown in Fig. 7. The heat-transfer coefficient h_o based on the tube outside diameter was calculated from the experimentally determined h_i and U. The overall heat-transfer coefficient U was determined by the following equation.

$$U = q\ \ln[(T_{pcm} - T_i)/(T_{pcm} - T_o)]/[\pi d_o L(T_o - T_i)], \quad (1)$$

where d_o, L, and T_{pcm} denote outside diameter of the tube, heat-transfer tube length, and the temperature of the PCM at the middle of heat-transfer tube and 37 mm apart from the surface in the radial direction, respectively.

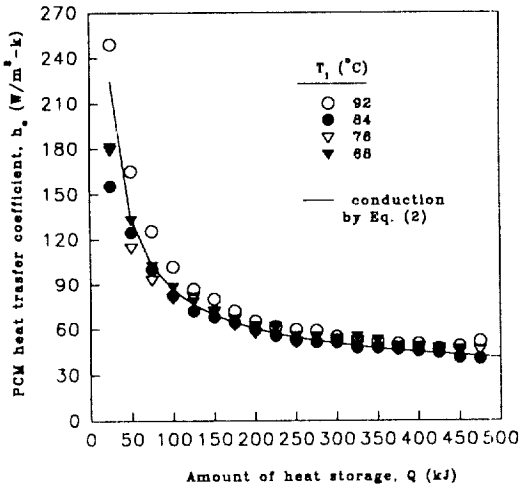

Fig. 7. PCM heat transfer coefficient with a variation of HTF inlet temperature in the unfinned-tube system (m=400 g/min).

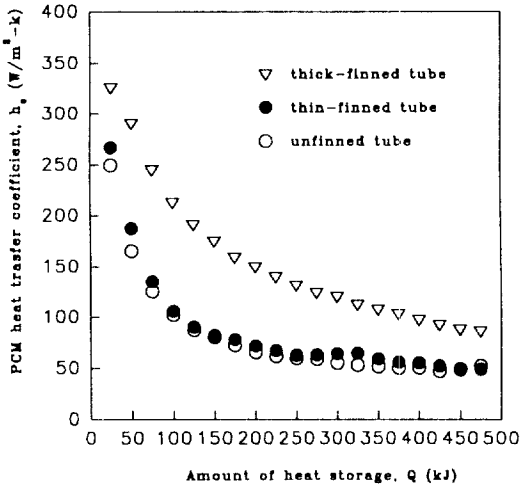

Fig. 8. Comparison of PCM heat transfer coefficients in three systems. (T_i=84℃, m=400 g/min)

On the other hand, for the unfinned tube system the heat-transfer coefficient h_o can be calculated from the steady-state conduction equation as follows.

$$h_o = 2\ k_l/[d_o\ \ln\ (d/d_o)], \tag{2}$$

where k_l and d are the thermal conductivity of melted PCM and the equivalent diameter of solid-liquid interface.

Furthermore, the equivalent diameter d_e can be calculated with the following equations.

$$d_e = [4\ V_l/(\pi L) + d_o^2]^{0.5}, \tag{3}$$

$$V_l = Q/\rho_l\lambda, \tag{4}$$

where ρ_l and λ are the density of the melted PCM and the latent heat of PCM.

In the Fig. 7 the solid line is calculated value from the Eq. (2) and heat transfer coefficients are plotted for the different inlet temperature of heat transfer fluid. As we expected from Eq. (2), the heat-transfer coefficient decreased with time due to the increased equivalent diameter of solid-liquid interface that increase the thermal resistance of conductive heat flux. It can be said that steady-state conduction equation can be applied with good accuracy for the prediction of heat-transfer coefficient of the unfinned-tube system in the heat storage stage. Above finding is contrary to the result of Yanadori and Masuda [Megerlin, 1967]. They reported that in the melting process heat transfer is largely influenced by natural convection. This difference may be caused by adding the thickening agent which is expected to suppress convective motion of the melted PCM.

Fig. 8 shows the comparison of heat-transfer coefficients for the three systems. Evidently the finned-tube system delivers higher heat flux thus higher heat-transfer coefficient than the unfinned-tube system due to the extended heat transfer surface. However for the thin finned-tube system the extended surface area (about 3 times larger heat transfer area than the unfinned-tube system) was not effective in enhancing the heat transfer. For the thick finned-tube system the enhanced heat transfer coefficient showed about 2 times higher than the unfinned-tube system. A more detail consideration and analysis should be given for evaluation of effective fin geometry and thickness.

3. Mathematical Analysis of Unfinned-tube System

The melting phenomenon of a solid PCM from an outside wall of the convective cooling unfinned-tube is modeled. Initially, the solid is assumed to be at its melting temperature, T_m. At time t=0, the temperature of the tube wall is suddenly increased by flowing the hot HTF through the inside tube. In the analysis, the following additional assumptions are made: (1) thermophysical properties of PCM undergoing phase change are independent of temperature. (2) volume change to the solid-liquid phase transition is negligible. (3) motion of natural convection in the melted PCM can be ignored. With the above assumptions, the position of solid-liquid interface (d/d_o) can be determined from the measured amount of heat storage (Q) and Eqs. (3) and (4). Let us define several important dimensionless groups in the analysis of the melting process.

$$\mathrm{Ste} = C_{pl}(T_w - T_m)/\lambda$$
$$\mathrm{Bi} = hx/k_l$$
$$\mathrm{Fo} = (k_l/\rho_l\ C_{pl})\ t/x_o^2$$
$$\eta^* = l/x_o$$
$$d\eta^*/d\mathrm{Fo} = d(d/d_o)/d\mathrm{Fo}$$
$$\theta = (T - T_m)/(T_b - T_m)$$

Dimensionless form of energy equation for the present system with boundary and initial conditions are given as:

$$\partial\theta/\partial F_o = \frac{1}{\eta}\frac{\partial}{\partial\eta}\left(\eta\frac{\partial\theta}{\partial\eta}\right) \quad \text{at } 1<\eta<\eta^* \tag{5}$$

$$\partial\theta/\partial\eta = -\mathrm{Bi}(1-\theta_w) \quad \text{at } \eta=1 \tag{6}$$

$$\theta = 0 \quad \text{at } \eta=\eta^* \tag{7}$$

$$-\mathrm{Ste}\frac{\partial\theta}{\partial\eta} = \partial\eta/\partial\theta = \eta^* \quad \text{at } \eta=\eta^* \tag{8}$$

$$\theta = 0 \quad \text{at Fo}=0 \tag{9}$$

The approximation solutions for the temperature distribution and the location of solid-liquid interface can be found elsewhere [Megerlin, 1967; Tao, 1967].

The effect of Biot number on melting front velocity is shown

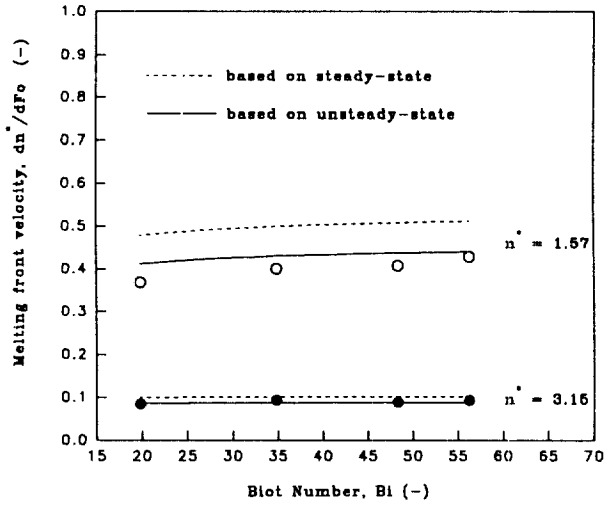

Fig. 9. Melting front velocity with a variation of Bi in the unfinned-tube system.
(Ste=0.376, T_i=84℃)

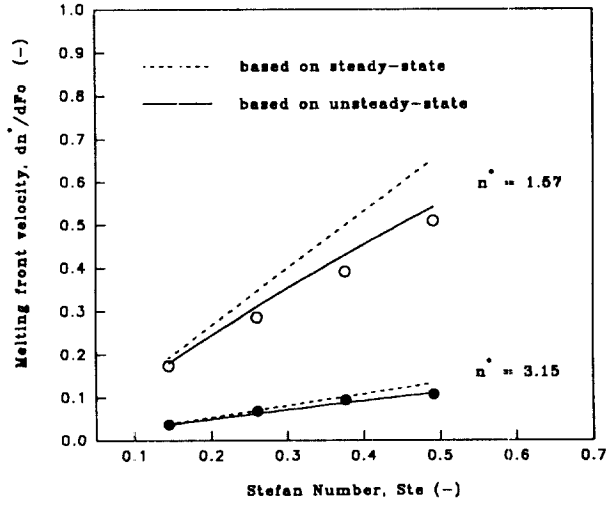

Fig. 10. Melting front velocity with a variation of Ste in the unfinned-tube system.
(Bi=34.8, m=400 g/min)

in Fig. 9. Two different analytical solutions were compared with experimental data. The solid line was calculated from Megerlin's approximation solution [Megerlin, 1967] and dotted line from Tao's quasi-stationary solution [Tao, 1967] (Laplace problem). As was mentioned before, the inside heat-transfer tube was inserted by spiral silicon wire which performs as a turbulence promoter it maintains higher heat-transfer coefficient for experimental ranges of flow rates of heat transfer fluid. Therefore in these operating conditions Biot numbers does not affect the melting front velocity at specific solid-liquid interface. The faster melting front velocity was obtained as the interface moves closer to the heat transfer surface due to the higher heat transfer coefficient at the beginning of heat storage stage. From the Fig. 9, it can be said that Megerlin's approximation gives more accurate prediction of moving front velocity than the simple quasi-stationary solution not only near the heat transfer surface but also far from the surface.

Fig. 10 shows the effect of Stefan number on melting front velocity. The dimensionless melting front velocity increased with Stefan number. The faster melting front velocity at the higher Stefan number at a certain radial position (η^*) is evident from the consideration of thermal driving force (ΔT) for heat transfer. The same theoretical approximations were used to compare with experimental data. As can be seen in the figure, Megerlin's unsteady-state approximation showed fairly good agreement with experimental results. The small difference of the melting front velocity between prediction and experimentally deduced values may results from the fact that the initial temperature of PCM was 5℃ lower than the melting point of PCM so that this sensible heat effect caused a little bit slower melting process at the beginning of heat storage stage. The fairly good agreement between predictions and experimental values at larger value of η^* (=3.15) where sensible heat effect is negligible confirmed the above reasoning.

4. Proposed Correlations for Melting Process

It is valuable to propose the correlations of melting process for unfinned and finned-tube systems with several dimensionless parameters that affect the heat storage characteristics. The experimental range employed in this study is expressed in terms of dimensionless groups as follows.

$0<Fo<40,\ 0.1<Ste<0.4,\ 330<Re<1300$

Two same types of correlations were obtained with 1500 data points for the unfinned-tube and the thick finned-tube system respectively.

For the unfinned-tube system

$$Q/Q_{max}=0.189\ Fo^{0.714}\ Ste^{0.561}\ Re^{0.011}, \tag{11}$$

and for the thick finned-tube system

$$Q/Q_{max}=0.406\ Fo^{0.726}\ Ste^{0.777}\ Re^{0.004} \tag{12}$$

The correlation coefficient of two equations was found to be in the range of 0.99. The proposed correlations showed that the thermal performance of this system is independent with flow rates of HTF. This results from the fact that the heat transfer of HTF side (h_i) is largely enhanced by the inserted turbulence promoter.

CONCLUSIONS

Sodium acetate trihydrate was employed as a potential material used for energy storage of low temperature energy source. In order to develop the efficient energy storage system, heat transfer characteristics for different heat transfer surface geometries and parameter effects on heat transfer were examined. This study has shown that the heat storage rate sharply decreased at the initial stage of heat storage and reached steady value for the rest of the stage. For the thick finned-tube system the rate of heat storage was measured to be 2 times higher than that for the unfinned-tube system. However for the thin finned-tube case, the heat transfer enhancement over unfinned tube was negligible. The heat-transfer coefficient based on the outside diameter of the heat-transfer tube was higher early in the melting process but fell off later and maintained steady value. The experimentally determined heat-transfer coefficients for the unfinned-tube and the thick finned-tube geometries were found to be in the range of 40-170 W/m^2-k, and 80-320 W/m^2-k, respectively. The theoretical unsteady-state conduction equation was found to be applicable reasonably to predict the melting front velocity for the unfinned-

tube system. The amount of heat storage of this study has been correlated in terms of the Fourier, Stefan and Reynolds numbers. The thermal performances are found to be strongly dependent on the inlet temperature of heat transfer fluid, as like in the heat recovery stage.

NOMENCLATURE

Bi : Biot number [-]
Cp_l : specific heat of liquid PCM [KJ/kg-k]
d : diameter of the solid-liquid interface [m]
d_e : equivalent diameter of the double tube [m]
d_o : outside diameter of heat transfer tube [m]
Fo : Fourier number, $4\alpha_l t/d_o$ [-]
G : mass velocity [kg/m^2-s]
h_i : fluid side heat-transfer coefficient [W/m^2 k]
h_o : PCM side heat-transfer coefficient [W/m^2 k]
k_l : thermal conductivity of liquid PCM [W/m k]
l : position of liquid-solid interface from tube center [m]
L : length of the heat-transfer tube [m]
m : flow rate of HTF [g/min]
q : heat transfer rate [W]
Q : total amount of heat storage [kJ]
Q_{max} : maximum capacity of heat storage [kJ]
Re : Reynold number, $d_e G/\mu$ [-]
Ste : Stefan number, $Cp_l (T_w - T_m)/\lambda$
T_i : inlet temperature of HTF [℃]
T_m : melting temperature of PCM [℃]
T_w : inside wall temperature of the heat transfer tube [℃]
V_l : volume of melted PCM [m^3]
x : distance from the tube center [m]
x_e : tube outside radius [m]

Greek Letters

α_l : thermal diffusivity of liquid PCM [m^2/sec]
λ : specific latent heat of PCM [kJ/kg]
ρ_l : liquid density of PCM [kg/m^3]
η : dimensionless distance
η^* : dimensionless distance of solid-liquid interface
θ : dimensionless temperature

REFERENCES

Abhat, A., "Low Temperature Latent Heat Material Energy Storage", *Solar Energy*, **30**, 313 (1983).

Lane, G. A., "Solar Heat Storage: Latent Heat Materials, Vol II, Technology", CRC Press, Florida (1986).

Megerlin, F., "Geometrisch Eindimesionale Waemeleitung Beim Schmelzen und Erstarren", *Forsch. Ing. Wes.*, **34**, 40 (1967).

Ryu, H. W., Woo, S. W., Shin, B. C. and Kim, S. D., "Prevention of Supercooling and Stabilization of Inorganic Salt Hydrate as Latent Heat Storage Materials", *Solar Energy Mat. Sol. Cells*, 161 (1992).

Shin, B. C., Kim, S. D. and Park, W. H., "Phase Separation and Supercooling of a Latent Heat Storage Materials", *Energy-The International Journal*, **14**, 921 (1989).

Tao, L. H., "Generallized Numerical Solution of Freezing a Saturated Liquid in Cylinders and Spheres", *AIChE J.*, **13**, 165 (1967).

Yanadori, M. and Masuda, T., "Heat Transfer Study on a Heat Storage Container with Phase Change Material", *Solar Energy*, **42**, 27 (1989).